Journal of Molecular Liquids 335 (2021) 116180

Contents lists available at ScienceDirect

Journal of Molecular Liquids

journal homepage: www.elsevier.com/locate/molliq

Molecular dynamics study on viscosities of sub/supercritical n-decane, n-undecane and n-dodecane

Xueming Yang [a,*], Mingli Zhang [a], Yue Gao [a], Jixiang Cui [a], Bingyang Cao [b,*]

[a] Department of Power Engineering, North China Electric Power University, Baoding 071003, China
[b] Key Laboratory for Thermal Science and Power Engineering of Ministry of Education, Department of Engineering Mechanics, Tsinghua University, Beijing 100084, China

a r t i c l e i n f o

Article history:
Received 20 December 2020
Revised 19 March 2021
Accepted 13 April 2021
Available online 17 April 2021

Keywords:
Alkanes
Viscosity
Molecular dynamic simulation
Surrogate fuel

a b s t r a c t

Viscosity is an essential property of fuels and a fundamental parameter in designing complex propulsion and power systems. In this paper, molecular dynamics (MD) simulations are conducted to compute viscosities of n-decane, n-undecane, and n-dodecane, Five force fields are compared by prediction of the viscosity. The results show that the MD predictions of the viscosity of the selected n-alkane are in good agreement with the reference data. In addition, the self-diffusion coefficient and radial distribution function of n-undecane are obtained from the MD simulations to better understand the viscosity characteristics of a sub/supercritical region at the molecular level. The Stokes-Einstein model and the Rouse model are employed to calculate the viscosity-temperature relationship of n-undecane under sub/supercritical conditions. It is found that the predicted viscosity values are significantly underestimated by the two models. This research offers reference for analyzing the thermophysical properties of N-alkanes and N-alkane-based fuels.

1. Introduction

Liquid alkane is an important fuel source [1–3] and a raw material of the modern chemical industry [4–6]. The flow characteristics of alkanes have been analyzed to determine the fundamental properties of petroleum and fuels since they are crucial for the heat transfer design of regenerative cooling of scramjets. Alkanes are commonly used propellants in propulsion and power systems [7,8] and can be used as a power source and a coolant to absorb heat from the air, reducing the temperature and consumption of cooling air. Viscosity is a crucial parameter in the design of the heat transfer and cooling system. However, it is challenging to determine viscosity experimentally and predict it accurately, especially for complex fluids composed of many molecules and under high-temperature and high-pressure conditions [9].

In recent years, molecular dynamics (MD) methods have become an important aspect of studying the transport properties of working fluids [10–14], molten salt [15–17] and refrigerant [18] and have attracted increasing attention from researchers. Payal et al. [19] used MD simulations to calculate the shear viscosity of n-decane and n-hexadecane with united atom and all-atomic force fields. The results showed that the calculated results of the united atom force field were within 20%-30% of the experimental value. Chen et al. [20] calculated the shear viscosity of n-dodecane at temperature of 660.15 K and pressures of 3 MPa, 10 MPa and 30 MPa using MD simulations; the errors compared with the experimental values are 20.23%, 13.03% and 22.31%, respectively. Zhang et al. [21] used the COMPASS force field to study the density and melting point of n-tetradecane, and their results were in good agreement with experimental data. Lee et al.[22] simulated the viscosity and self-diffusion coefficient of four normal alkanes (C12, C20, C32, and C44); the simulation and experimental results were in good agreement. Nicolas et al. [23] calculated the surface tension of linear alkanes (n-hexane, n-decane, and n-hexadecane) with different force fields, and the calculation results obtained by the SKS force field differs from the experimental results by about 15%. Kondratyuk et al. [24] adopted MD simulations to calculate the diffusion coefficient of n-triacontane, the average absolute deviation between the results and the experimental data is 21.4%.

Many MD simulations studies were performed on the viscosity of n-decane[19,23], dodecane[20,25], and other straight-chain alkanes [22,24]. However, to the best of our knowledge, there are no reports of MD studies on the viscosity characteristics of n-undecane. In fact, N-decane, n-undecane, and n-dodecane have been used as components in surrogate mixture for aviation

* Corresponding authors.
E-mail addresses: xuemingyang@ncepu.edu.cn (X. Yang), caoby@tsinghua.edu.cn (B. Cao).

https://doi.org/10.1016/j.molliq.2021.116180
0167-7322/

kerosene under subcritical and supercritical conditions in MD studies to analyze the properties of aviation kerosene in the regeneration cooling system and the engine injection system, thus it is necessary to investigate the MD calculations of the viscosity characteristics of n-undecane systematically.

The transport properties of a fluid can be obtained from equilibrium molecular dynamics (EMD) and non-equilibrium molecular dynamics (NEMD) simulations. Kondratyuk et al. [26] concluded that both methods give consistent results at pressure less than 100 MPa.

In this study, equilibrium MD (EMD) simulations with different force field models are conducted to compare the viscosity of n-decane, n-undecane, and n-dodecane and systematically analyze the transport characteristics and local structures of n-undecane. The rest of this article is organized as follows. Section 2 describes the model construction and simulation method and details. Section 3 presents the MD simulation results and the size effect and comparisons of the force field models. Structural analyses and theoretical calculations are performed to understand the viscosity of n-undecane at the molecular level. The numerical data and uncertainty estimates are provided in the supplementary material to allow readers to compare the obtained calculations.

2. Method

2.1. Green-Kubo formula

The Green-Kubo formula is used to calculate the viscosity of the selected three alkanes. This formula relates viscosity to the stress-stress normalized autocorrelation function (NACF). The NACF is calculated in the three coordinate directions and averaged to improve the accuracy of the results. The shear viscosity can be calculated as follows [27]:

$$\eta = \frac{V}{k_B T}\int_0^\infty \sum_a \sum_b \left\langle P_{ab}(t)\cdot P_{ab}(0)\right\rangle dt \quad (1)$$

where η is the shear viscosity, V and T denote the volume and the temperature of the system, respectively. k_B is the Boltzmann constant, which is $1.3806504 \times 10^{-23}$ J/K. a and b denote the x-, y-, and z-directions in Cartesian coordinates (a – b). The angle bracket < > denotes the average of the autocorrelation function.$P_{ab}(t)$represents the pressure tensor components in the a- and b-directions at time t and is calculated as follows[27]:

$$P_{ab}(t) = \frac{1}{V}\left[\sum_i^N m_i v_{ia} v_{ib} + \sum_{i=1}^{N-1}\sum_{j>1}^{N} r_{ija} f_{ijb}\right] \quad (2)$$

where N is the number of molecules,m_i is the mass of a molecule i. $v_{ia}$and v_{ib} are the velocity components of a molecule i in the a- and b-directions, and r and f represent the displacement and force between two molecules, respectively.

2.2. Force field models

In this paper, the following potential energy model is adopted: [26]

$$E = E_{bond} + E_{angle} + E_{dihedral} + E_{improper} + E_{Vdw} + E_{coul} \quad (3)$$

where E_{bond} is the bond interaction; $E_{angle}$is the angular interaction; $E_{dihedral}$is the interaction of dihedral angles;$E_{improper}$is the interaction of non-dihedral angles; $E_{Vdw}$and E_{coul} are the van der Waals forces and Coulomb forces between molecules, respectively. Five force field models are compared in this study, including the AMBER model [28], OPLS/AA model [29], L-OPLS model [30], COMPASS model [31], and TraPPE-UA model [32]. The well-known Lorentz-Berthelot mixing rule [27] is used to describe the interactions between different atoms in the system [33].

Table 1
The characteristic of n-decane, n-undecane, and n-dodecane.

Molecular name	Relative molecular weight	Critical temperature/ K	Critical pressure/ MPa
N-decane ($C_{10}H_{22}$)	142.28	617.7	2.103
N-undecane($C_{11}H_{24}$)	156.31	638.8	1.990
N-dodecane($C_{12}H_{26}$)	170.33	658.1	1.817

2.3. Molecular simulation details

The relative molecular weight, critical temperature, critical pressure and molecular structures of the selected alkanes are shown in Table 1 and Fig. 1.

The EMD simulations are carried out using the Large-scale Atomic/Molecular Massively Parallel Simulator (LAMMPS) software package [34]. A three-dimensional cubic simulation box is used with periodic boundary conditions in all directions. A typical simulation system for $C_{11}H_{24}$ (total molecular number N = 250) is shown in Fig. 2.

The particle–particle/particle-mesh (PPPM) [35] is used to calculate the long-range electrostatic interaction [36,37]. The cutoff distance of the Lennard-Jones (LJ) interactions is 12 Å [20,26],

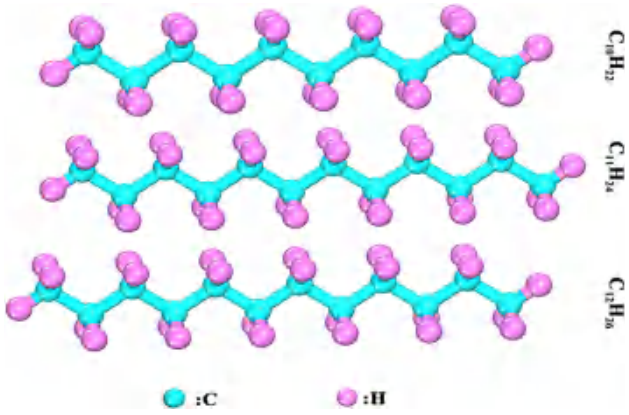

Fig. 1. (color online). Molecular structure of n-decane, n-undecane, and n-dodecane.

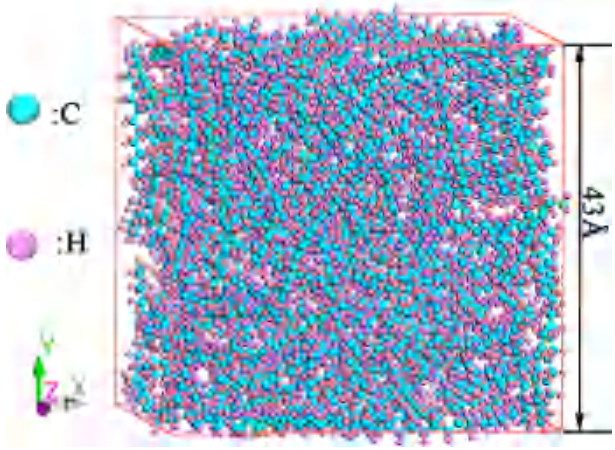

Fig. 2. (color online). The simulation box consisted of 250 $C_{11}H_{24}$ molecular.

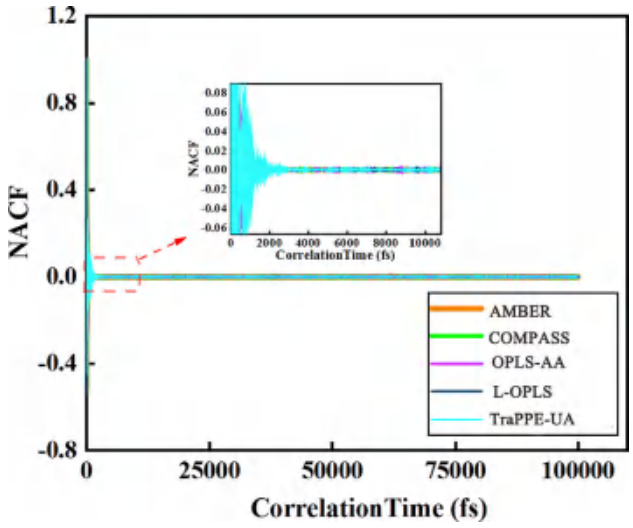

Fig. 3. (color online). The calculated NACF for five selected force fields.

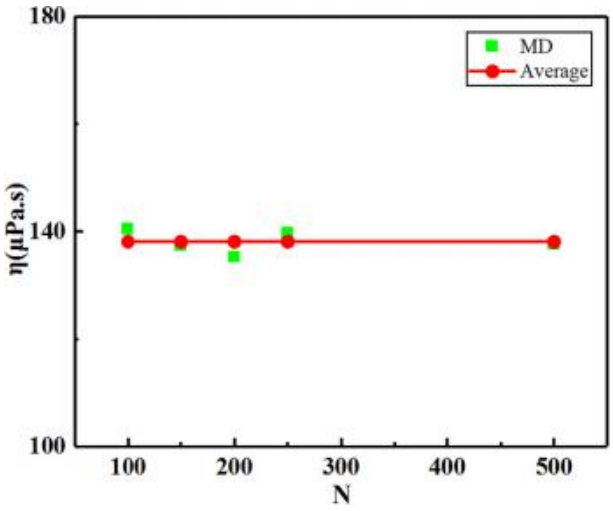

Fig. 4. (color online). Viscosity obtained from the EMD simulation for n-decane with different system sizes.

and the time step is 0.4 fs. During the simulations, the system initially runs under an NPT ensemble to maintain the system pressure and equilibrium for 1 ns at a given pressure. Subsequently, then an NVT ensemble is applied to the system for 1 ns at a given temperature. Finally, the viscosity is calculated in the NVT ensemble for 2 ns or longer for production.

2.4. Effect of system size in predicting viscosity

We conduct six independent simulations by changing initial velocity to obtain a reliable value result of the viscosity. The viscosity at a given temperature and pressure is estimated by averaging the values of the six independent runs, and the error estimates are obtained by calculating the standard error of the values. The NACF is calculated to determine the correlation time S. We choose the value of S when NACF has decayed completely and converged almost to zero in the simulation. The EMD simulation strategy for the viscosity calculation is similar to that in our previous studies [11,38]. Fig. 3 shows the NACF of n-decane for different force field models. The NACF of n-decane is calculated at a pressure of 3 MPa and a temperature of 500 K. It is observed that the NACFs for different force fields are similar and decay to zero relatively quickly (within 3000 fs). This means correlation time 3000 fs is enough for the convergence of NACF to zero for different force fields , thus in our EMD simulations, the correlation time of the EMD simulations are chosen as 3000 fs.

In order to test the influence of the number of molecules during EMD simulations, five different numbers of molecules (100, 150, 200, 250, and 500 molecules) are studied at pressure of 3 MPa and temperature of 500 K to determine the influence of the system size, as shown in Fig. 4. The prediction results of the five simulation box sizes are shown in Fig. 4. The green dots represent the simulation results of the tested five simulated boxes, while the solid line represents the averaged viscosity. These results conclude that size of the system has a negligible effect on viscosity when the number of molecules exceeds 100.

3. Results and discussion

3.1. The selection and comparison of the force field models

At present, the commonly used force field models for long-chain alkanes include AMBER, OPLS/AA, L-OPLS, COMPASS and TraPPE-UA models[20,21,24,25,38]. Therefore, we compare these five force field models for the transport characteristics of alkanes. Here, the viscosity of pure n-decane from the NIST database is used as a reference to obtain the accurate force field model [40–44]. In this study, five different force field models are compared, and the viscosity and mass density of n-decane at 3 MPa pressure and temperatures from 350 K to 600 K are obtained from the EMD simulations. The results are shown and compared with the NIST data in Fig. 5(a) and 5(b).

The absolute relative error (ARE) between the MD simulation results and the corresponding NIST data is calculated as follows:

$$\mathrm{ARE} = \left| \frac{g_{\mathrm{Sim}} - g_{\mathrm{NIST}}}{g_{\mathrm{NIST}}} \right| \times 100\% \quad (4)$$

where g_{Sim} and g_{NIST} represent the MD and the NIST viscosities, respectively. The AREs corresponding to the results in Fig. 5(a) and (b) are shown in Figs. 6 and 7, respectively. To evaluate the prediction accuracy, AREs of the force field models at all temperatures tested are averaged. The COMPASS model exhibits the best performance for predicting viscosity and mass density. The averaged AREs of the COMPASS model for viscosities and densities at temperatures from 350 K to 600 K are 13.88% and 3.77%, respectively. These results are consistent with an earlier study made by Kondratyuk et al. [39], who found that the COMPASS force field had the best performance for predicting viscosity of 2-pyrrine-4-trimethylpentane compare to OPLS-AA and L-OPLS force field models. Compared to the AMBER, OPLS-AA and L-OPLS force fields models, the main difference is that all the cross terms between bonds, angles, dihedrals are included in COMPASS force field model. TraPPE-UA model is a typical UA model in which each CH_2 and CH_3 in alkane is simplified by a pseudoatom. Thus we guess that the COMPASS model could capture the viscosity behaviors of the alkane in more detail, thus result in a good performance in prediction of the viscosities. This suggests the COMPASS model as an accurate force field model to predict viscosity of n-decane ($C_{10}H_{22}$), n-undecane ($C_{11}H_{24}$), and n-dodecane ($C_{12}H_{26}$). Thus in the following simulations, only the COMPASS model is used to predict the viscosity.

3.2. Simulation results of different alkanes

The viscosities and densities of n-decane ($C_{10}H_{22}$), n-undecane ($C_{11}H_{24}$), and n-dodecane ($C_{12}H_{26}$) are calculated at pressure of 3 MPa and five selected temperatures using the EMD simulations.

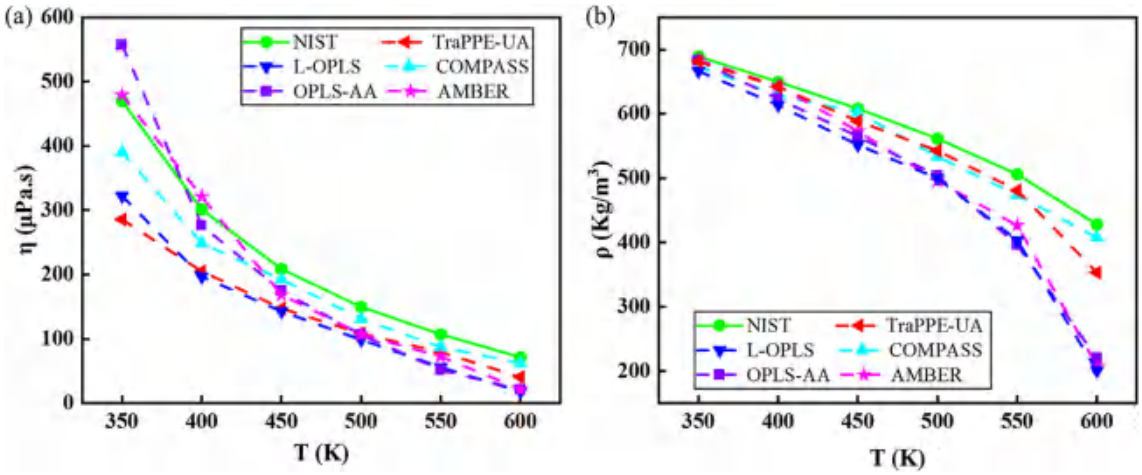

Fig. 5. (color online). (a) The viscosity and (b) mass density as a function of the temperature obtained from the EMD simulations with five different force field models.

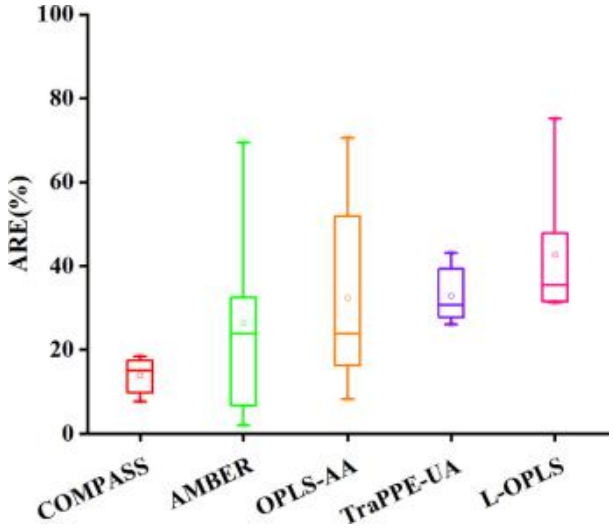

Fig. 6. (color online). AREs of the viscosity obtained from EMD simulations with five different force field models at temperatures from 350 K to 600 K.

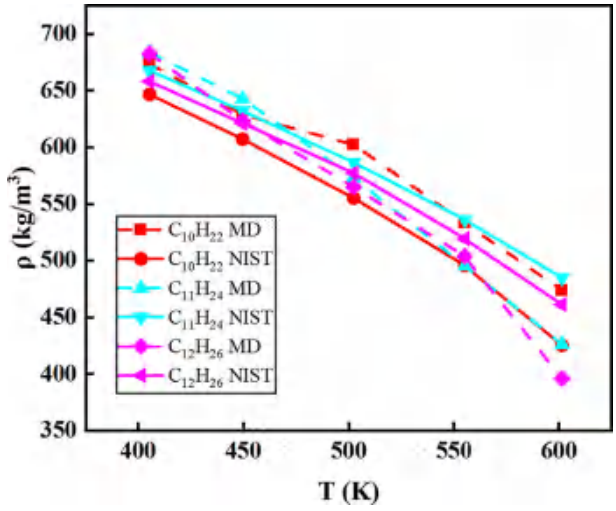

Fig. 8. (color online). The mass density as a function of the temperature obtained from EMD simulations with different alkanes.

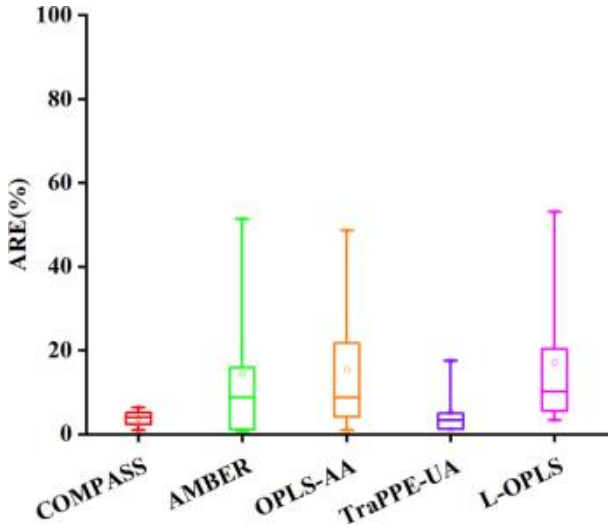

Fig. 7. (color online). AREs of the density obtained from EMD simulations with five different force field models at temperatures from 350 K to 600 K.

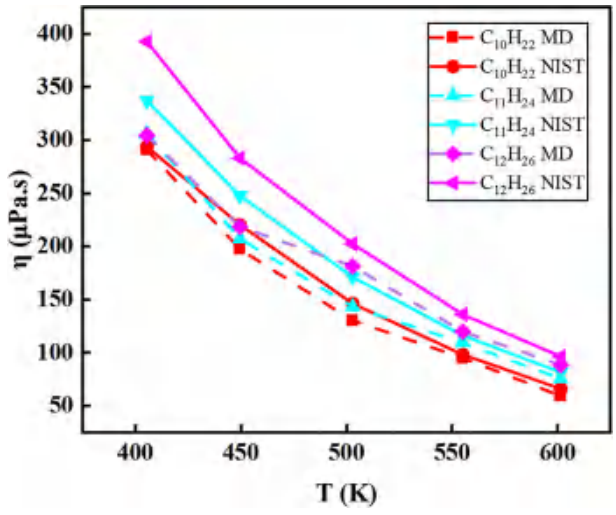

Fig. 9. (color online). The viscosity as a function of the temperature obtained from EMD simulations for three different alkanes.

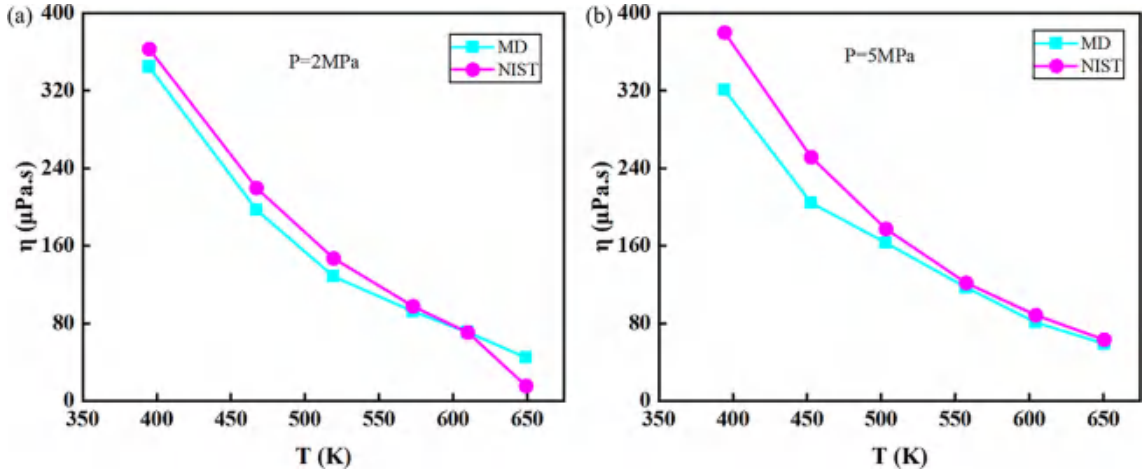

Fig. 10. (color online). Viscosity as a function of temperature obtained from EMD simulations of $C_{11}H_{24}$ at (a) Pressure of 2 MPa , and (b) Pressure of 5 MPa.

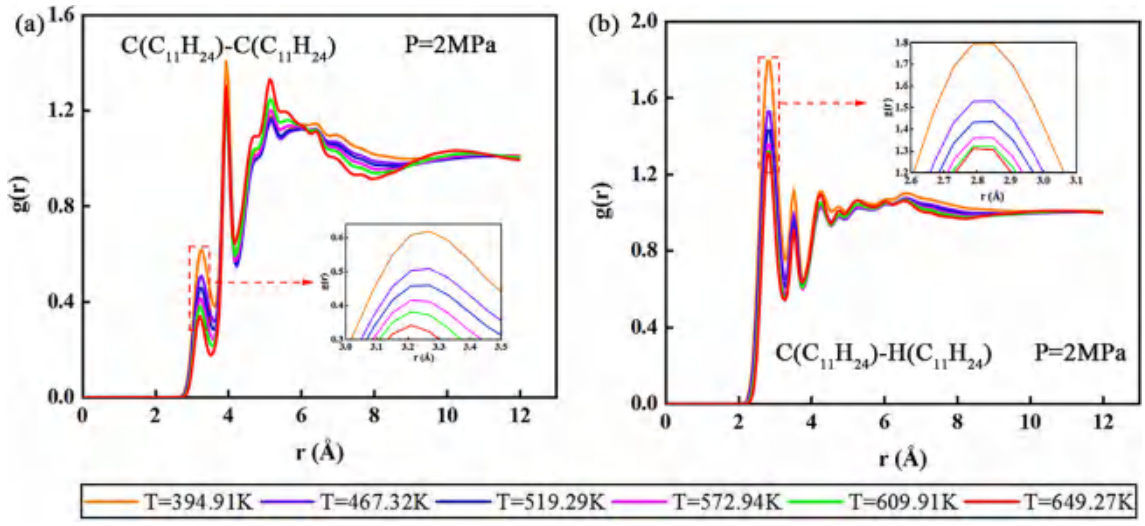

Fig. 11. (color online). RDF of different atom types for $C_{11}H_{24}$ at pressure of 2 MPa: (a) $C(C_{11}H_{24})$-$C(C_{11}H_{24})$ and (b) $C(C_{11}H_{24})$-$H(C_{11}H_{24})$.

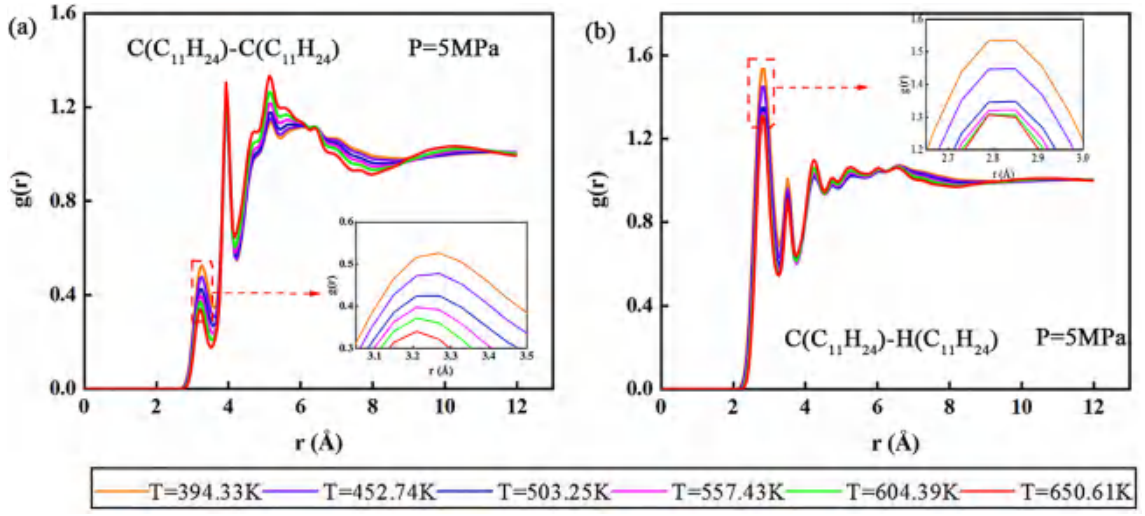

Fig. 12. (color online). RDF of different atom types for $C_{11}H_{24}$ at pressure of 5 MPa: (a) $C(C_{11}H_{24})$-$C(C_{11}H_{24})$ and (b) $C(C_{11}H_{24})$-$H(C_{11}H_{24})$.

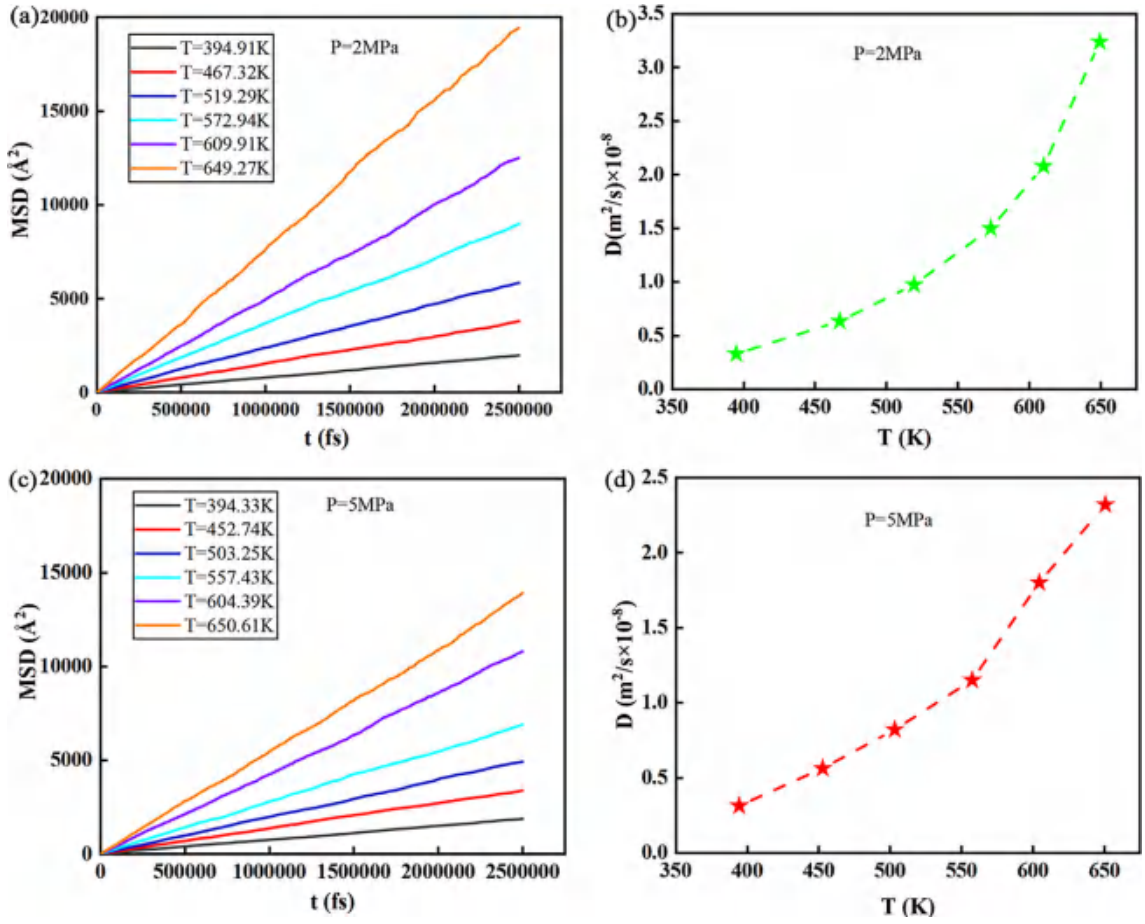

Fig. 13. (color online). The MSD and the self-diffusion coefficient (D) of $C_{11}H_{24}$.

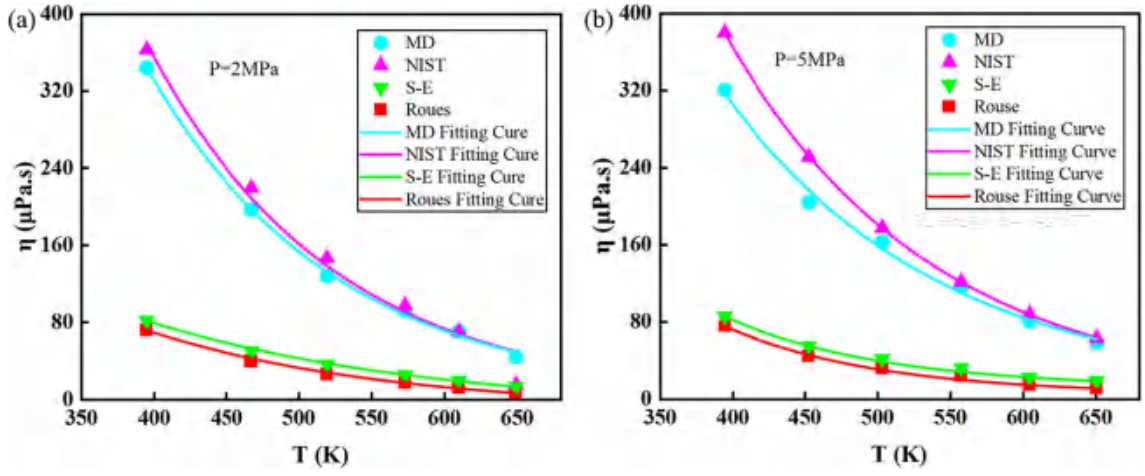

Fig. 14. (color online). The fitted viscosity-temperature curves obtained from the MD simulations, NIST data, S-E model, and Rouse model at (a) pressure of 2 MPa, and (b) pressure of 5 MPa.

It should be noted that the temperature values selected are the same as those used in Refs. [45–47] for RP-3 aviation kerosene. Thus, our results can be used in future investigations of aviation kerosene substitutes. The simulation results are shown in Figs. 8 and 9, respectively, and are compared with the NIST data. The AREs of the predicted densities and viscosities at all temperatures tested are averaged for each alkane. The averaged AREs for predicting the density of $C_{10}H_{22}$, $C_{11}H_{24}$, and $C_{12}H_{26}$ are 7.02%, 5.22% and 4.67%, respectively, and the averaged ARE for predicting the viscosity are 7.16%, 11.03% and 15.17%, respectively. The corresponding data (including NIST data) are listed in Tables S6 and S8 in the supplementary material. Figs. 8 and 9 show that the viscosity and density decrease when temperatures increase at constant pressure.

A special effort is made to calculate viscosity of n-undecane under sub/supercritical conditions, since no MD studies were conducted to date. Fig. 10 describe the calculated viscosities of $C_{11}H_{24}$,

which agree very well with the NIST data at pressures of 2 MPa and 5 MPa and the five selected temperatures. The trend of the viscosity obtained from the simulation is the same as that of NIST, showing a gradual decrease with an increase in the temperature. Under subcritical states (2 MPa), the averaged AREs of $C_{11}H_{24}$ at temperatures tested is 6.82% (excluded the value near the critical point, T = 638.8 K, P = 1.990 MPa). However, at T = 649.27 K and P = 2 MPa, the ARE of the viscosity is relatively large (189.48%). Large errors in predicted viscosity values near the critical point have been observed in previous EMD simulation studies [20,25,48]. In fact, it is still quite challenging to accurately predict the thermophysical properties of fluids near or at the critical point by using MD simulations, and further research efforts should be made. Under supercritical conditions (5 MPa), the averaged ARE at all temperatures tested is 10.28%. These results demonstrate that the EMD simulations with the COMPASS force field model provide acceptable predictions for the viscosity of n-decane, n-undecane, and n-dodecane at subcritical and supercritical states.

3.3. Structural analysis

The radial distribution function (RDF) g(r) represents the probability of finding another particle at a certain distance r from a reference particle. It is the ratio of the local density of the system at the reference particle to the average density of the entire system, reflecting the aggregation of molecules in the liquid and the internal structure of the liquid.

$$g_{ab}(r) = \frac{1}{4\pi\rho_b r^2}\left[\frac{dN_{ab}(r)}{dr}\right] \tag{5}$$

where ρ_b is the numerical density of the b particles.N_{ab} is the number of b particles in a sphere with a particles in the center and radius r. In general, the first peak of g(r) represents the aggregation degree between the atoms or molecules in the first neighborhood.

The RDFs of n-undecane ($C_{11}H_{24}$) are shown in Figs. 11 and 12, respectively, in the two states (sub/supercritical) (1) P = 2 MPa, T = 390–650 K and (2) P = 5 MPa, T = 390–650 K. It is observed that at different temperatures, $g(r)_{C(C_{11}H_{24})-C(C_{11}H_{24})}$has three peaks located at 3.2 Å, 3.93 Å, and 5.13 Å, respectively. The three peaks of $g(r)_{C(C_{11}H_{24})-H(C_{11}H_{24})}$ are observed at 2.8 Å, 3.5 Å, and 4.28 Å, respectively. The local magnification of the first peak shows that the peak values of $g(r)_{C(C_{11}H_{24})-C(C_{11}H_{24})}$ and $g(r)_{C(C_{11}H_{24})-H(C_{11}H_{24})}$decrease gradually with an increase in the temperature, indicating that the aggregation degree of the $C_{11}H_{24}$ molecules decreases as the temperature increases in the subcritical and supercritical states. The amplitude of the first peaks of $g(r)_{C(C_{11}H_{24})-H(C_{11}H_{24})}$is much higher than those of $g(r)_{C(C_{11}H_{24})-C(C_{11}H_{24})}$ at the same temperatures and pressure. The RDF analysis shows that the aggregation degree and the viscosity of the n-undecane molecules decrease with an increase in the temperature.

3.4. Self-diffusion coefficient (D)

The self-diffusion coefficient is calculated to determine the viscosity characteristics of n-undecane. The self-diffusion coefficient is calculated using the time-dependent mean square displacement (MSD) as follows:

$$D = \frac{1}{6N}\lim_{t\to\infty}\frac{d}{dt}\left\langle\sum_{i=1}^{N}[r_i(t) - r_i(0)]^2\right\rangle \tag{6}$$

where $r_i(t)$and$r_i(0)$ are the positions of molecule i at time t and 0. $\langle\sum_{i=1}^{N}[r_i(t) - r_i(0)]^2\rangle$ is the MSD. The MSD of $C_{11}H_{24}$ is calculated based on the EMD simulations for (1) P = 2 MPa, T = 350–650 K and (2) P = 5 MPa, T = 350–650 K, see Fig. 13(a) and 13(c). The slope of the MSD increases as the temperature increases. The self-diffusion coefficient D is calculated based on the MSD value using Eq. (6), as shown in Fig. 13(b) and 13(d). It is observed that the self-diffusion coefficient D increases non-linearly with increasing temperature.

3.5. Stokes-Einstein model and Rouse model

The Stokes-Einstein (S-E) model and the Rouse model have been widely used for the theoretical calculation of fluid viscosities[49]. The S-E equation describes the relationship between the self-diffusion coefficient D and the viscosity as follows:

$$\eta = \frac{2K_BT}{\pi C_{SE} d D} \tag{7}$$

where d is the hydrodynamic diameter, and C_{SE} is the S-E coefficient. C_{SE} = 6 for the stick boundary condition and C_{SE} = 4 for the slip boundary condition. The Rouse model [50] was initially used to estimate the viscosity of polymers that fit the Gaussian chain. When the long-chain molecule satisfies the formula of the Gaussian chain $<R^2>=6<R_g>=nb^2$, R is the distance between the ends of the molecular chain (Å); $R_g$is the radius of gyration (Å); b is the effective bond length. The Rouse model is calculated as follows:

$$\eta(R_g) = \frac{\rho RTR_g^2}{6MD} \tag{8}$$

where $\eta(R_g)$is the viscosity of the system Pa.s; ρ is the density of the system, kg/m^3, R is the molar gas constant, 8.314 J/ (mol.K); T is the temperature of the system, K,R_g is the radius of rotation, m; M is the molar mass, kg/mol; D is the diffusion coefficient, m^2/s.

The viscosity-temperature fitting curves obtained from the MD, NIST, S-E model, and Rouse model are shown in Fig. 14. The fitting curves for pressure of 2 MPa and 5 MPa as table2. It is observed that the MD simulation values agree relatively well with the NIST values. The values calculated by the S-E model and Rouse model are similar, and the trends of the viscosity-temperature curves are the same as those of the MD simulations and NIST data. However, both the S-E model and the Rouse model significantly underestimated the viscosity. In the calculation of the S-E model, it is found that computed values of $D\eta/T$ are changed with temperatures, as shown in Table 3. This means $D\eta/T$does not remain constant, which indicates the breakdown of the S-E relationship [51,52]. The underestimations of the Rouse model for the

Table 2
The fitting curves for pressure of 2 MPa and 5 MPa.

	2 MPa	5 MPa
η_{MD}	$7081{:}48 \cdot e^{-0{:}008T}$	$3999{:}50 \cdot e^{-0{:}007T}$
η_{NIST}	$8246{:}98 \cdot e^{-0{:}008T}$	$5957{:}70 \cdot e^{-0{:}007T}$
η_{S-E}	$1145{:}70 \cdot e^{-0{:}008T}$	$970{:}20 \cdot e^{-0{:}007T}$
η_{Rouse}	$1922{:}31 \cdot e^{-0{:}008T}$	$1531{:}37 \cdot e^{-0{:}007T}$

Table 3
The calculated the $D\eta/T$for the $C_{11}H_{24}$.

P(MPa)	T(K)	$D\eta/T(m^2 \cdot Pa \cdot K^{-1})$
2 MPa	394.91	0.288×10^{-14}
	467.32	0.268×10^{-14}
	519.29	0.241×10^{-14}
	572.94	0.241×10^{-14}
	609.91	0.242×10^{-14}
	649.27	0.222×10^{-14}

viscosities prediction of n-undecane viscosity are resulted from the short chain of n-undecane which can not satisfy the Gaussian chain [50,53]. These results indicate that the S-E model and Rouse model are not suitable for calculating and predicting the viscosity-temperature relationship of $C_{11}H_{24}$.

4. Conclusions

In this study, the viscosities of sub/supercritical n-decane, n-undecane, and n-dodecane are systematically analyzed using the EMD method. EMD simulation models for predicting the viscosities are established, and five force field models (AMBER, OPLS/AA, L-OPLS, COMPASS, and TraPPE-UA) are compared to determine the optimum force field for viscosity prediction. It is found that the COMPASS force field shows the best performance for viscosity prediction, and the EMD simulation results are in agreement with the NIST reference data. Additionally, the self-diffusion coefficient and RDF of n-undecane are obtained from the MD simulations to better understand the viscosity characteristics of the sub/supercritical region at the molecular level. The results show that the aggregation degree of the n-undecane molecules decreases with an increase in the temperature, decreasing the viscosity. The S-E model and the Rouse model are used to calculate the viscosity-temperature relationship of n-undecane under subcritical/supercritical conditions. The viscosity values are significantly underestimated by these two models. The research results can provide reference data for analyzing the thermophysical properties of fuels based on n-alkanes.

CRediT authorship contribution statement

Xueming Yang: Conceptualization, Methodology, Validation, Writing - original draft. Mingli Zhang: Investigation, Writing - review & editing. Yue Gao: Visualization, Validation. Jixiang Cui: . Bingyang Cao: Supervision, Software.

Declaration of Competing Interest

The authors declare that they have no known competing financial interests or personal relationships that could have appeared to influence the work reported in this paper.

Acknowledgments

This research is supported by the National Science and Technology Major Project (Grant No. 2017-III-0005-0030) and the National Key R&D Program of china (Grant No. 2016YFB0600100).

Appendix A. Supplementary material

Supplementary data to this article can be found online at https://doi.org/10.1016/j.molliq.2021.116180.

References

[1] D. Kim, J. Martz, A. Violi, A surrogate for emulating the physical and chemical properties of conventional jet fuel, Combust. Flame 161 (6) (2014) 1489–1498.
[2] P. Wang, Z. Dong, Y. Tan, Z. Liu, Investigating the Interactions of the Saturate, Aromatic, Resin, and Asphaltene Four Fractions in Asphalt Binders by Molecular Simulations, Energy Fuels 29 (1) (2015) 112–121.
[3] T. Edwards, Surrogate Mixtures to Represent Complex Aviation and Rocket Fuels, J. Propul. Power 2 (17) (2001) 461–466.
[4] L. Zhang, M.L. Greenfield, Analyzing Properties of Model Asphalts Using Molecular Simulation, Energy Fuels 21 (3) (2007) 1712–1716.
[5] C. McCabe, S. Cui, P.T. Cummings, Characterizing the viscosity–temperature dependence of lubricants by molecular simulation, Fluid Phase Equilib. 183 (2001) 363–370.
[6] J.H. Dymond, K.J. Young, Transport properties of nonelectrolyte liquid mixtures—I. Viscosity coefficients for n-alkane mixtures at saturation pressure from 283 to 378 K, Int. J. Thermophys. 1 (4) (1980) 331–344.
[7] T. Edwards, Liquid Fuels and Propellants for Aerospace Propulsion: 1903–2003, J. Propul. Power 19 (6) (2003) 1089–1107.
[8] B. Palaszewski, L.S. Ianovski, P. Carrick, Propellant Technologies: Far-Reaching Benefits for Aeronautical and Space-Vehicle Propulsion, J. Propul. Power 14 (5) (1998) 641–648.
[9] Y. Yang, T.A. Pakkanen, R.L. Rowley, NEMD Simulations of Viscosity and Viscosity Index for Lubricant-Size Model Molecules, Int. J. Thermophys. 23 (6) (2002) 1441–1454.
[10] X. Yang, J. Xu, S. Wu, M. Yu, B. Hu, B. Cao, J. Li, A molecular dynamics simulation study of PVT properties for $H_2O/H_2/CO_2$ mixtures in near-critical and supercritical regions of water, Int. J. Hydrogen Energy 43 (24) (2018) 10980–10990.
[11] X. Yang, C. Duan, J. Xu, Y. Liu, B. Cao, A numerical study on the thermal conductivity of $H_2O/CO_2/H_2$ mixtures in supercritical regions of water for coal supercritical water gasification system, Int. J. Heat Mass Transf. 135 (2019) 413–424.
[12] X. Yang, Y. Feng, J. Jin, Y. Liu, B. Cao, Molecular dynamics simulation and theoretical study on heat capacities of supercritical H_2O/CO_2 mixtures, J. Mol. Liq. 299 (2020) 112133.
[13] A. Alkhwaji, S. Elbahloul, M.Z. Abdullah, K.F.B.A. Bakar, Selected water thermal properties from molecular dynamics for engineering purposes, J. Mol. Liq. 114703 (2020).
[14] J. Nichele, A.B. de Oliveira, L.S.D.B. Alves, I. Borges, Accurate calculation of near-critical heat capacities C_P and C_V of argon using molecular dynamics, J. Mol. Liq. 237 (2017) 65–70.
[15] B. Li, S. Dai, D. Jiang, Molecular dynamics simulations of structural and transport properties of molten NaCl-UCl3 using the polarizable-ion model, J. Mol. Liq. 299 (2020) 112184.
[16] J. Wang, C. Liu, Temperature and composition dependences of shear viscosities for molten alkali metal chloride binary systems by molecular dynamics simulation, J. Mol. Liq. 273 (2019) 447–454.
[17] X. Guo, H. Qian, J. Dai, W. Liu, J. Hu, R. Shen, J. Wang, Theoretical evaluation of microscopic structural and macroscopic thermo-physical properties of molten AF-ThF4 systems (A+ = Li+, Na+ and K+), J. Mol. Liq. 277 (2019) 409–417.
[18] M.S. Alam, J.H. Jeong, Molecular dynamics simulations on homogeneous condensation of R600a refrigerant, J. Mol. Liq. 261 (2018) 492–502.
[19] R.S. Payal, S. Balasubramanian, I. Rudra, K. Tandon, I. Mahlke, D. Doyle, R. Cracknell, Shear viscosity of linear alkanes through molecular simulations: quantitative tests for n-decane and n-hexadecane, Mol. Simul. 38 (14–15) (2012) 1234–1241.
[20] C. Chen, X. Jiang, Y. Sui, Prediction of transport properties of fuels in supercritical conditions by molecular dynamics simulation, Energy Procedia 158 (2019) 1700–1705.
[21] Zhang Xuelai et al., Molecular dynamics simulation of the phase transition process of n-tetradecane, Energy Storage Sci. Technology 8 (05) (2019) 874–879.
[22] S.H. Lee, T. Chang, Viscosity and Diffusion Constants Calculation of n-Alkanes by Molecular Dynamics Simulations, Bull. Korean Chem. Soc. 24 (11) (2003) 1590–1598.
[23] J.P. Nicolas, B. Smit, Molecular dynamics simulations of the surface tension of n-hexane, n-decane and n-hexadecane, Mol. Phys. 100 (15) (2002) 2471–2475.
[24] N.D. Kondratyuk, G.E. Norman, V.V. Stegailov, Rheology of liquid n-triacontane: Molecular dynamics simulation, J. Phys. Conf. Ser. 774 (2016) 12039.
[25] C. Chen, X. Jiang, Transport property prediction and inhomogeneity analysis of supercritical n-Dodecane by molecular dynamics simulation, Fuel 244 (2019) 48–60.
[26] N.D. Kondratyuk, V.V. Pisarev, Calculation of viscosities of branched alkanes from 0.1 to 1000 MPa by molecular dynamics methods using COMPASS force field, Fluid Phase Equilib. 498 (2019) 151–159.
[27] M.P. Allen, D.J. Tildesley, Computer simulation of liquids, Oxford University Press, 1989.
[28] S.J. Weiner, P.A. Kollman, D.A. Case, U.C. Singh, C. Ghio, G. Alagona, S. Profeta, P. Weiner, A new force field for molecular mechanical simulation of nucleic acids and proteins, J. Am. Chem. Soc. 106 (3) (1984) 765–784.
[29] K. Kahn, T.C. Bruice, Parameterization of OPLS-AA force field for the conformational analysis of macrocyclic polyketides, J. Comput. Chem. 23 (10) (2002) 977–996.
[30] S.W.I. Siu, K. Pluhackova, R.A. Böckmann, Optimization of the OPLS-AA Force Field for Long Hydrocarbons, J. Chem. Theory Comput. 8 (4) (2012) 1459–1470.
[31] H. Sun, COMPASS: An ab Initio Force-Field Optimized for Condensed-Phase ApplicationsOverview with Details on Alkane and Benzene Compounds, J. Phys. Chem. B 102 (38) (1998) 7338–7364.
[32] L. Zhang, J.I. Siepmann, Pressure Dependence of the Vapor−Liquid−Liquid Phase Behavior in Ternary Mixtures Consisting of n-Alkanes, n-Perfluoroalkanes, and Carbon Dioxide, J. Phys. Chem. B 109 (7) (2005) 2911–2919.
[33] T. Akıner, H. Ertürk, K. Atalık, Prediction of Thermal Conductivity and Shear Viscosity of Water-CU Nanofluids Using Equilibrium Molecular Dynamics, Proceedings of the ASME 2013 International Mechanical Engineering Congress and Exposition (2013).
[34] S. Plimpton, Fast Parallel Algorithms for Short-Range Molecular Dynamics, J. Comput. Phys. 117 (1) (1995) 1–19.

[35] M.S. Kelkar, J.L. Rafferty, E.J. Maginn, J. Ilja Siepmann, Prediction of viscosities and vapor–liquid equilibria for five polyhydric alcohols by molecular simulation, Fluid Phase Equilib. 260 (2) (2007) 218–231.
[36] M.J. Stevens, M. Mondello, G.S. Grest, S.T. Cui, H.D. Cochran, P.T. Cummings, Comparison of shear flow of hexadecane in a confined geometry and in bulk, J. Chem. Phys. 106 (17) (1997) 7303–7314.
[37] Y. Zhang, A. Otani, E.J. Maginn, Reliable Viscosity Calculation from Equilibrium Molecular Dynamics Simulations: A Time Decomposition Method, J. Chem. Theory Comput. 11 (8) (2015) 3537–3546.
[38] X. Yang, Y. Feng, J. Xu, J. Jin, Y. Liu, B. Cao, Numerical study on transport properties of the working mixtures for coal supercritical water gasification based power generation systems, Appl. Therm. Eng. 162 (2019) 114–228.
[39] N.D. Kondratyuk, Comparing different force fields by viscosity prediction for branched alkane at 0.1 and 400 MPa, J. Phys. Conf. Ser. 1 (1385) (2019).
[40] F. Xue, Analysis of Thermal Properties of Daqing RP-3 Aviation Kerosene, J. Propulsion Technology 02 (27) (2006) 187–192.
[41] F.L.C.X. Guoxin Dang, Numerical study on flow and convection heat transfer characteristics of supercritical kerosene, Science China Press 03 (43) (2013) 440–446.
[42] X. Hui, C.J. Sung, Laminar flame speeds of transportation-relevant hydrocarbons and jet fuels at elevated temperatures and pressures, Fuel 01 (109) (2013) 191–200.
[43] I.M. Abdulagatov, L.A. Akhmedova-Azizova, Viscosity of rocket propellant (RP-1) at high temperatures and high pressures, Fuel 235 (2019) 703–714.
[44] E.W. Lemmon, M.L. Huber, Thermodynamic Properties of n-Dodecane, Energy Fuels 18 (4) (2004) 960–967.
[45] H.W. Deng, C.B. Zhang, G.Q. Xu, Z. Tao, B. Zhang, G.Z. Liu, Density Measurements of Endothermic Hydrocarbon Fuel at Sub- and Supercritical Conditions, J. Chem. Eng. Data 56 (6) (2011) 2980–2986.
[46] H.W. Deng, C.B. Zhang, G.Q. Xu, B. Zhang, Z. Tao, K. Zhu, Viscosity Measurements of Endothermic Hydrocarbon Fuel from (298 to 788) K under Supercritical Pressure Conditions, J. Chem. Eng. Data 57 (2) (2011) 358–365.
[47] X.G.D.H. Jia Zhouxia, Dynamic viscosity measurement of aviation kerosene RP-3 under subcritical pressure, J. Beijing University Aeronautics Astronautics 07 (40) (2014) 934–938.
[48] J.C. Phys, Transport properties of carbon dioxide and methane from molecular dynamics simulations, J. Chem. Phys. 141 (2016), 134101.
[49] S.R. Ecker, P.H. Poole, F.W. Starr, Fractional Stokes-Einstein and Debye-Stokes-Einstein relations in a network-forming liquid, Phys. Rev. Lett. 5 (97) (2006) 2–5.
[50] M. Mondello, G.S. Grest, E.B. Webb, P. Peczak, Dynamics of n-alkanes: Comparison to Rouse model, J. Chem. Phys. 2 (109) (1998) 798–805.
[51] W.J. Lamb, G.A. Hoffman, J. Jonas, Self-diffusion in compressed supercritical water, J. Chem. Phys. 74 (12) (1981) 6875–6880.
[52] P. Bordat, F. Affouard, M. Descamps, F. Müller-Plathe, The breakdown of the Stokes-Einstein relation in supercooled binary liquids, J. Phys.: Condens. Matter 15 (32) (2003) 5397–5407.
[53] M. Mondello, G.S. Grest, Viscosity calculations of n-alkanes by equilibrium molecular dynamics, J. Chem. Phys. 22 (106) (1997) 9327–9336.